Ultrasound and Photoacoustic Imaging of Peripheral Arteries

A Feasibility Study

Chandramoorthi, Sowmiya; Thomas, Anjali; van Soest, Gijs; Francis, Kalloor Joseph

DOI
10.1016/j.ultrasmedbio.2025.06.001

Publication date
2025

Document Version
Final published version

Published in
Ultrasound in Medicine and Biology

Ultrasound in Medicine & Biology 51 (2025) 1854–1858

Contents lists available at ScienceDirect

Ultrasound in Medicine & Biology

journal homepage: www.elsevier.com/locate/ultrasmedbio

Technical Note

Ultrasound and Photoacoustic Imaging of Peripheral Arteries: A Feasibility Study

Sowmiya Chandramoorthi [a], Anjali Thomas [b], Gijs van Soest [b,c,d], Kalloor Joseph Francis [b,*]

[a] Verasonics Inc, Kirkland, WA, USA
[b] Department of Cardiology, Thorax Center, Cardiovascular Institute, Erasmus University Medical Center, Rotterdam, The Netherlands
[c] Department of Precision and Microsystems Engineering, Delft University of Technology, Delft, The Netherlands
[d] Wellman Center for Photomedicine, Massachusetts General Hospital, Boston, MA, USA

ARTICLE INFO

Keywords:
Photoacoustic imaging
Atherosclerosis
Carotid artery
Femoral artery
Ultrasound imaging

ABSTRACT

Photoacoustic imaging of the arteries can provide valuable functional information to diagnose and classify atherosclerotic plaques. When combined with ultrasound for anatomical information, photoacoustic imaging holds promise for routine monitoring and for treatment decisions. However, utilizing conventional ultrasound systems for combined photoacoustic and ultrasound imaging has not been successful for this application. In this study, we imaged two major arteries susceptible to atherosclerosis—the carotid artery and the femoral artery—using a linear array-based system. Our results demonstrate the feasibility of imaging the carotid artery at depths of up to 10 mm and the femoral arteries at up to 20 mm. The average success rates for imaging the carotid, common femoral and superficial femoral arteries in healthy volunteers were 75%, 100% and 33.3%, respectively, demonstrating potential for future studies.

Introduction

Atherosclerosis is a systemic disease of the arteries that affects millions of people worldwide. It can cause cardiovascular events, such as limb ischemia, myocardial infarction and stroke [1]. Accurate diagnosis of atherosclerosis is crucial for timely treatment and effective management. Imaging modalities, such as Doppler ultrasound (US) and magnetic resonance angiography, provide information on stenosis and blood flow but have limitations in quantifying plaque composition to identify plaque risk [2,3]. Non-invasive photoacoustic (PA) imaging of atherosclerosis, used in combination with conventional US assessment of the vasculature, adds contrast to pathophysiology, as revealed in plaque tissue composition.

Femoral plaque formation can limit blood flow to the leg, causing intermittent claudication. This form of peripheral artery disease can eventually cause critical limb ischemia, leading to necrosis and possibly amputation. If exercise therapy is unsuccessful, revascularization by minimally invasive or surgical plaque removal (atherectomy), or bypass surgery, may be necessary [4]. Currently, only morphological parameters, such as diameter or area stenosis and lesion length, are considered in treatment decisions. Plaque composition may be predictive of the long-term success of atherectomy, and could support the choice between a minimally invasive approach and surgery. In addition, studies have shown that intima-media thickness in the femoral artery can be an early indicator of cardiovascular disease [3,5–7]. Refinement of this metric with plaque composition could support the development of precision cardiovascular risk assessment based on non-invasive femoral plaque imaging.

In the carotid artery, endarterectomy is a surgical procedure in which plaque is removed from the artery, and symptomatic patients with severe carotid artery disease are eligible for this treatment [8,9]. However, the current patient-selection protocol depends only on the degree of arterial stenosis, while the hallmarks of plaque vulnerability are not taken into account [10]. In this context, combined US and PA imaging can be valuable for routine imaging, evaluating both stenosis and plaque composition for vulnerability tests and in treatment planning [11].

Imaging of the carotid artery has previously been explored, primarily utilizing custom-developed handheld probes. The early feasibility of non-invasive carotid imaging using a concave US transducer was demonstrated in human volunteers [12]. Ivankovic et al. used a handheld multispectral optoacoustic tomography volumetric scanner from iThera Medical (Munich, Germany) to demonstrate real-time anatomical and functional imaging of the carotid bifurcation [13]. Karlas et al. applied spectral unmixing, differentiating lipid and hemoglobin content to

* Corresponding author. Department of Cardiology, Thorax Center, Cardiovascular Institute, Erasmus University Medical Center, Dr. Molewaterplein 40, 3015 GD Rotterdam, The Netherlands.
E-mail address: f.kalloorjoseph@erasmusmc.nl (K.J. Francis).
Sowmiya Chandramoorthi and Anjali Thomas contributed equally to this manuscript.

https://doi.org/10.1016/j.ultrasmedbio.2025.06.001
Received 9 April 2025; Revised 30 May 2025; Accepted 3 June 2025

distinguish healthy from atherosclerotic carotid arteries [14]. Intraoperative imaging using a linear array US transducer and a laser diode as the light source was investigated by Muller et al., who improved the signal-to-noise ratio by compensating for motion artifacts during plaque imaging [15]. Steinkamp et al. further advanced PA imaging using molecular contrast agents targeting vascular endothelial growth factor to visualize atherosclerotic plaques [16]. Preliminary results demonstrated PA imaging of the jugular vein using a linear array US transducer integrated into a commercial Philips US system [17]. These studies highlight the potential of combined US and PA imaging for carotid artery pathology. However, the femoral artery has not been imaged before using PA techniques, in spite of being an important target for the early indication of atherosclerosis. Optimizing conventional US systems for PA imaging of peripheral arteries also remains a challenge. Factors such as receiver sensitivity and signal-to-noise ratio, which in turn affect the imaging depth, are important considerations.

In this work, we demonstrated the use of a linear array-based system optimized for imaging major arteries of the peripheral circulation and demonstrated PA imaging of the femoral and carotid arteries in four healthy volunteers. This study shows real-time handheld imaging of major arteries situated at a depth of 10–20 mm, paving the way for clinical studies of tissue composition in peripheral artery atherosclerotic disease. These advances are enabled by the use of a new programmable US platform with a high-impedance front end and adjustable gain.

Materials and methods

Combined PA and US imaging was performed using a Verasonics Vantage NXT 256 HF system (Kirkland, WA, USA). The system has a 16-bit analog-to-digital converter resolution and a sampling rate of 125 MHz. A receive gain of 48 dB (low-noise amplifier + programmable amplifier gain) was set on the system during passive reception, along with an active termination of 1500 Ω and a receive filter bandwidth of 100%, centered around the transducer frequency. The system was synchronized with a Photosonus X100 laser source (Ekspla, Lithuania) operating at a repetition rate of 100 Hz, which triggered the NXT system upon each laser pulse. We employed single-wavelength illumination at 870 nm, targeting oxygenated hemoglobin within the artery, to demonstrate the feasibility. The laser output was coupled to a bifurcated slit fiber positioned at an angle of 37 degrees to the transducer, ensuring that the beams intersected at a distance of 15 mm from the probe in free space. A custom-printed holder was used to align and secure the transducer and slit fibers together as a handheld probe. In this study, the laser pulse energy was adjusted to maintain an output fluence of 4.6 mJ/cm^2 at the skin surface in contact with the transducer, which is below the maximum permissible exposure defined by IEC 60825-1 standards. We employed a L12-3v US transducer that has 192 elements and operates at a center frequency of 7.54 MHz. This transducer requires a MUXed dual-aperture acquisition when used in combination with a 128-channel connector of the NXT system. Therefore, two laser pulses are needed per acquisition, resulting in a maximum achievable frame rate of 50 Hz. A total of 50 image frames were acquired during each experiment from one volunteer. Each frame contained a set of B-mode US and PA data. B-mode US images were acquired using plane wave compounding with five steered angles.

Four healthy volunteers, aged between 25 and 36 years, participated in the *in vivo* experiments after providing informed consent under study protocol MEC-2014-611. Both longitudinal and cross-sectional images of the common carotid artery (CCA) and common femoral artery (CFA), and longitudinal images of the superficial femoral artery (SFA), were acquired. For carotid artery imaging, volunteers were placed in a sitting position to minimize the diameter of the jugular vein. After identification of the carotid artery using US imaging, volunteers were instructed to tilt their heads to displace the sternocleidomastoid muscle superiorly,

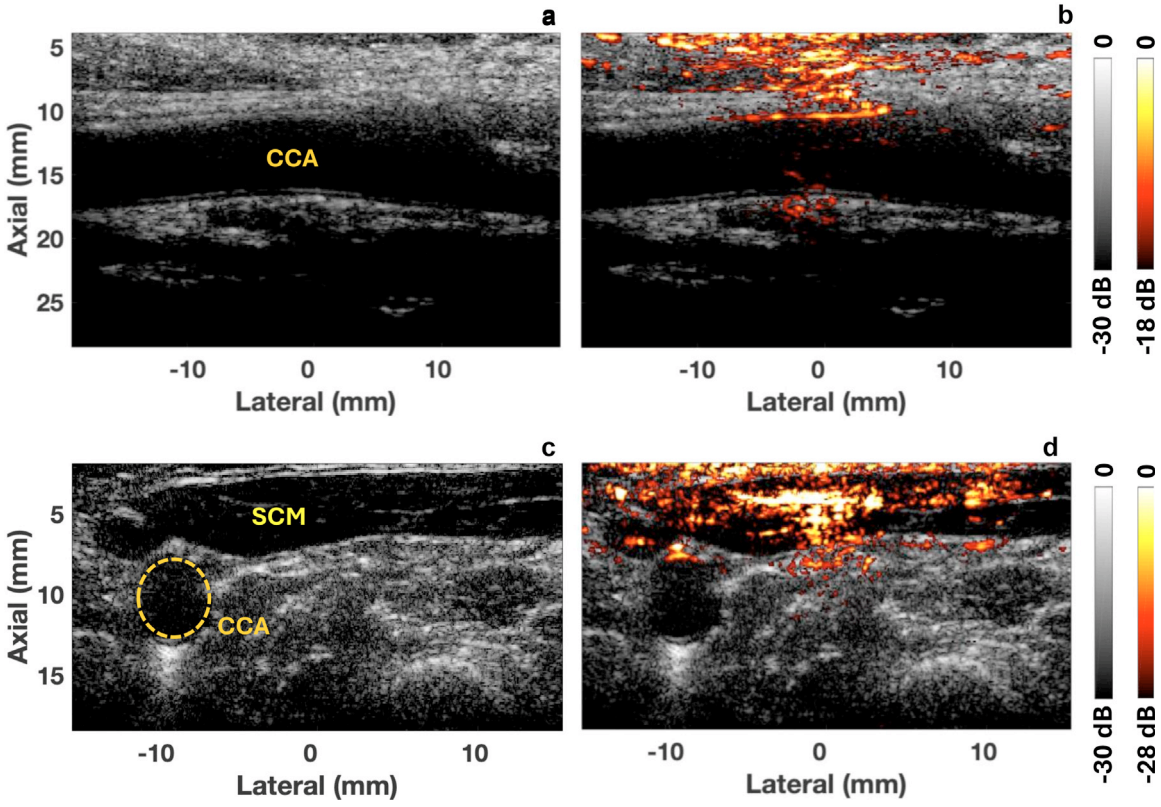

Figure 1. Carotid artery imaging. (a) Longitudinal ultrasound (US) image of the common carotid artery (CCA) and (b) corresponding photoacoustic image overlaid on top of the US image. (c) Cross-sectional US image showing the sternocleidomastoid (SCM) muscle and the CCA and (d) overlaid photoacoustic image. SCM.

Table 1
Analysis of imaging showing depth achieved and signal-to-noise ratio.

Volunteer			CCA		CFA	
No.	Age (years)	Sex	Depth range (mm)	SNR range (dB)	Depth range (mm)	SNR range (dB)
1	34	F	8–10	6–17	15–20	11–19
2	36	M	ND	ND	7–18	15–20
3	27	F	5–8	12–20	6–15	12–19
4	36	F	6.5–10	8–13	NA	NA

CCA, common carotid artery; CFA, common femoral artery; NA, not applicable; ND, not detected.

optimizing light delivery to the artery. Once the optimal position was established, the light source was activated using a foot pedal switch, and simultaneous PA and US images were recorded. For femoral artery imaging, volunteers were positioned supine on an examination bed. Following identification with US imaging, combined PA and US images of CFA and SFA were acquired.

Results and discussion

Figure 1 shows US and PA images of the CCA obtained from Volunteer 1 (Fig. 1a, 1b) and Volunteer 3 (Fig. 1c, 1d). Figure 1 (a, b) presents longitudinal views of the CCA, while Figure 1 (c, d) shows cross-sectional views. The carotid lumen appears hypoechoic in US imaging,

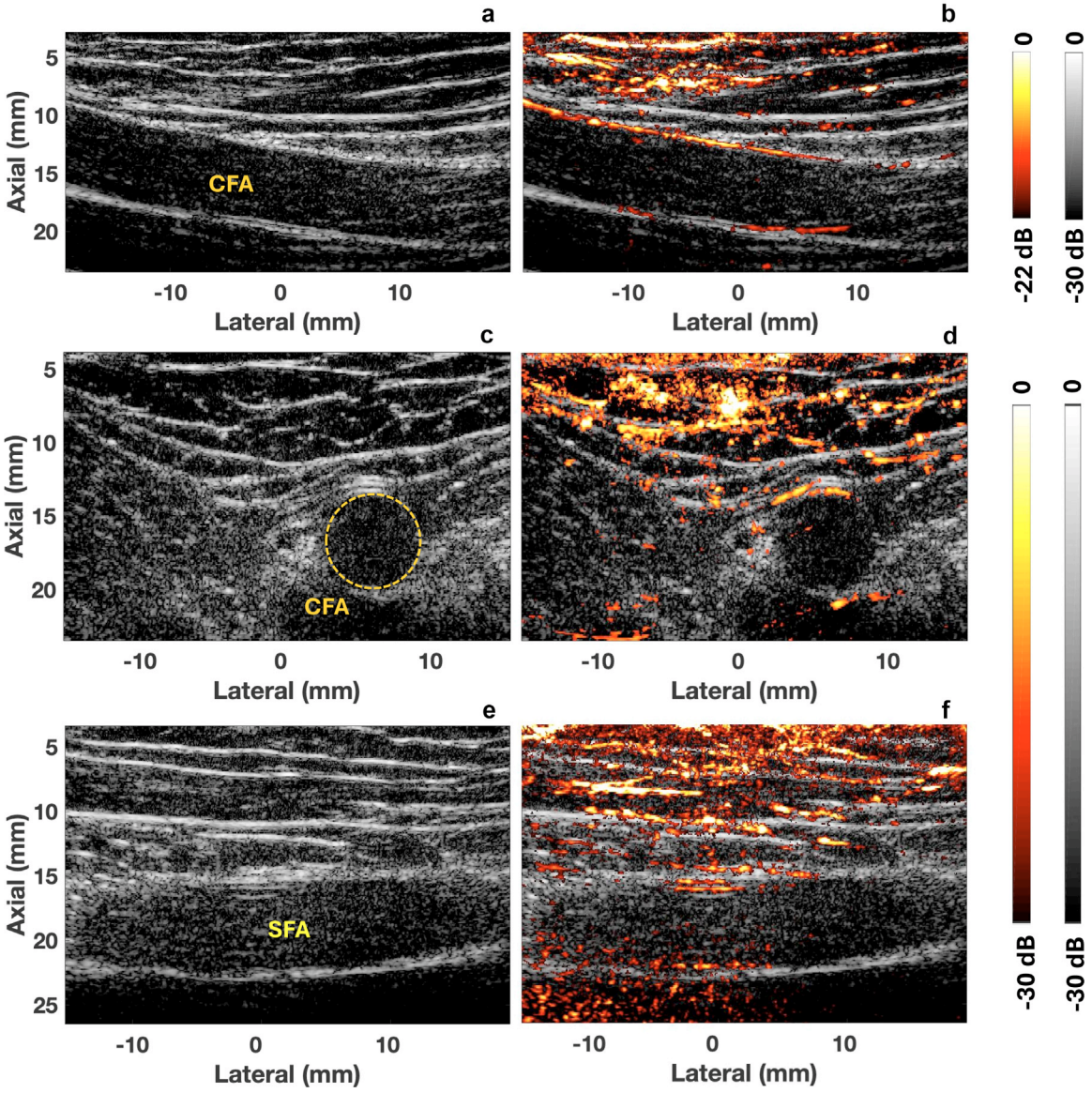

Figure 2. Femoral artery imaging. (a) Longitudinal ultrasound (US) image of the common femoral artery (CFA) and (b) corresponding overlaid photoacoustic image. Cross-section of the CFA (c) US image and (d) overlaid PA image. (e) Longitudinal US image of the superficial femoral artery (SFA) and (f) overlaid photoacoustic image.

while PA signals originating from blood are primarily visible near the vessel boundaries due to the limited bandwidth of the transducer. Near-field clutter was observed in the PA images, being more prominent in cross-sectional views compared with longitudinal views. This difference may result from reduced interference from superficial structures, such as the sternocleidomastoid muscle, and better illumination conditions in the longitudinal imaging orientation. In this study, the carotid artery was successfully imaged up to a maximum depth of 10 mm, achieving a signal-to-noise ratio (SNR) greater than 6 dB. Table 1 provides details on age, sex, the depth range at which the artery is found when imaging the artery from different locations and the SNR range of targets for images acquired in different trials for a particular volunteer. PA imaging of the CCA was successful in three out of four volunteers (success rate of 75%), with one case unsuccessful due to limitations in imaging depth. Several factors influenced imaging success, including artery depth, anatomical obstacles (such as muscle tissue or the jugular vein), and skin pigmentation, as higher melanin levels reduced fluence and increased noise.

Figure 2 shows US and PA images of the femoral artery of Volunteer 2. Figure 2 (a, b) illustrates longitudinal views of the CFA, while Figure 2 (c, d) displays cross-sectional views of the CFA. Figure 2 (e, f) depicts longitudinal views of the SFA. The top boundary of the CFA was clearly visible (Fig. 2a, 2b), and a portion of its bottom edge at approximately 17 mm depth was also detected. Figure 2d demonstrates the CFA positioned between 15 and 20 mm depth, showing detectable PA signals from its upper boundary. Only three volunteers participated in the femoral artery imaging study and the CFA was located between 6 and 20 mm below the skin surface. More details of the CFA imaging of volunteers can be found in Table 1. These results confirm that PA signals can be obtained *in vivo* from the CFA at depths up to 20 mm with an SNR greater than 11 dB. PA images were successfully obtained in all three volunteers, achieving a success rate of 100%.

Imaging the SFA proved more challenging compared with the CFA due to interference from the sartorius muscle located anterior to the artery. Nevertheless, measurable PA signals from the SFA were detected in Volunteer 2, with the upper boundary of the artery identified at a depth of 16 mm and its lower boundary at 22 mm (Fig. 2e, 2f).

Beyond 22 mm, increased background noise prevented the extraction of useful information; thus, SFA imaging was not successful in the other two volunteers for this reason.

Clutter, notably in the cross-sectional PA images, indicates that factors such as skin melanin concentration, illumination angle and superficial anatomy substantially affected image quality. Thus, optimizing probe design, imaging protocols and developing clutter-removal techniques are essential. Hardware enhancements, such as optimizing the orientation of the fiber optic bundle relative to the US transducer, have been shown to improve both penetration depth and SNR [18]. Multi-wavelength imaging can further aid clutter reduction by leveraging the distinct spectral signatures of different tissue components [19]. In addition, advanced imaging protocols such as localized vibration tagging and deformation-compensated averaging [20,21], and several post processing techniques [22,23], have been explored as promising methods for further clutter suppression in photoacoustic imaging.

Additionally, previous studies have demonstrated that multi-wavelength photoacoustic imaging can identify lipid deposits and intra-plaque hemorrhage, both of which are markers of plaque vulnerability [14,24]. While not explored in this study, it should be considered for plaque assessment. The PA signals observed originate from the blood pool within the arterial lumen and appear exclusively at the blood −artery wall interface. This artifact arises due to the limited low-frequency response of the US transducer and significant optical attenuation in blood. Enhancing the transducer's low-frequency bandwidth could improve image fidelity [25]. Additionally, heterogeneity of atherosclerotic plaques, the primary imaging target, results in increased high-frequency signal generation [26].

Conclusion

This study successfully demonstrates the potential of combined US and photoacoustic imaging for imaging peripheral arteries, potentially detecting vulnerable atherosclerotic plaques in the carotid and femoral arteries. Further technical advancements in probe optimization and clutter removal could result in the clinical utility of this combined imaging approach.

Conflict of interest

S.C. is an employee of Verasonics Inc., which supported this study. G. v.S. is a cofounder of, and has equity in, Kaminari Medical BV, who were not involved in the submitted work. In the past 3 years, he was the PI on research projects, administered by Erasmus MC, that received research support from FUJIFILM VisualSonics, Shenzhen Vivolight, Boston Scientific, Waters and Mindray (outside the submitted work). The other authors have no conflicts of interest to disclose.

Acknowledgments

This work was supported by the Dutch Research Council NWO-VICI (16131), NWO-VENI (19165) and Verasonics, Inc.

Author contributions

Sowmiya Chandramoorthi: Conceptualization, methodology, investigation, formal analysis, writing − original draft; Anjali Thomas: Conceptualization, methodology, investigation, formal analysis, writing − original draft; Gijs van Soest: Conceptualization, methodology, writing − review and editing, supervision; Kalloor Joseph Francis: Conceptualization, methodology, writing − review and editing, supervision.

Data availability statement

The data are available from the corresponding author upon request.

References

[1] Martin SS, Aday AW, Almarzooq ZI, Anderson CA, Arora P, Avery CL, et al. 2024 heart disease and stroke statistics: a report of US and global data from the American Heart Association. Circulation 2024;149:e347–913.
[2] Poznyak AV, Sukhorukov VN, Eremin II, Nadelyaeva II, Orekhov AN. Diagnostics of atherosclerosis: overview of the existing methods. Front Cardiovasc Med 2023;10:1134097.
[3] Nielsen RV, Fuster V, Bundgaard H, Fuster JJ, Johri AM, Kofoed KF, et al. Personalized intervention based on early detection of atherosclerosis: JACC state-of-the-art review. J Am Coll Cardiol 2024;83:2112–27.
[4] Beckman JA, Schneider PA, Conte MS. Advances in revascularization for peripheral artery disease: revascularization in PAD. Circ Res 2021;128:1885–912.
[5] Khoury Z, Schwartz R, Gottlieb S, Chenzbraun A, Stern S, Keren A. Relation of coronary artery disease to atherosclerotic disease in the aorta, carotid, and femoral arteries evaluated by ultrasound. Am J Cardiol 1997;80:1429–33.
[6] Schmidt C, Fagerberg B, Hulthe J. Non-stenotic echolucent ultrasound-assessed femoral artery plaques are predictive for future cardiovascular events in middle-aged men. Atherosclerosis 2005;181:125–30.
[7] Lucatelli P, Fagnani C, Tarnoki AD, Tarnoki DL, Stazi MA, Salemi M, et al. Femoral artery ultrasound examination: a new role in predicting cardiovascular risk. Angiology 2017;68:257–65.
[8] Hsu HY, Lin CJ, Lee YS, Wu TH, Chien KL. Efficacy of more intensive lipid-lowering therapy on cardiovascular diseases: a systematic review and meta-analysis. BMC Cardiovasc Disord 2020;20:1–12.
[9] Rathenborg LK. Should we be (even more) restrictive in selecting patients for carotid endarterectomy? Eur J Vasc Endovasc Surg 2020;59:525.
[10] Bos D, van Dam-Nolen DH, Gupta A, Saba L, Saloner D, Wasserman BA, et al. Advances in multimodality carotid plaque imaging: AJR expert panel narrative review. Am J Roentgenol 2021;217:16–26.
[11] Kruizinga P, van der Steen AF, de Jong N, Springeling G, Robertus JL, van der Lugt A, et al. Photoacoustic imaging of carotid artery atherosclerosis. J Biomed Opt 2014;19 110504−110504.
[12] Dima A, Ntziachristos V. Non-invasive carotid imaging using optoacoustic tomography. Opt Express 2012;20:25044–57.

[13] Ivankovic I, Mercep E, Schmedt CG, Dean-Ben XL, Razansky D. Real-time volumetric assessment of the human carotid artery: handheld multispectral optoacoustic tomography. Radiology 2019;291:45–50.
[14] Karlas A, Kallmayer M, Bariotakis M, Fasoula NA, Liapis E, Hyafil F, et al. Multispectral optoacoustic tomography of lipid and hemoglobin contrast in human carotid atherosclerosis. Photoacoustics 2021;23:100283.
[15] Muller JW, van Hees R, van Sambeek M, Boutouyrie P, Rutten M, Brands P, et al. Towards *in vivo* photoacoustic imaging of vulnerable plaques in the carotid artery. Biomed Opt Express 2021;12:4207–18.
[16] Steinkamp PJ, Vonk J, Huisman LA, Meersma GJ, Diercks GF, Hillebrands JL, et al. VEGF-targeted multispectral optoacoustic tomography and fluorescence molecular imaging in human carotid atherosclerotic plaques. Diagnostics 2021;11:1227.
[17] Garcia-Uribe A, Erpelding TN, Ke H, Reddy KN, Sharma A, Wang LV. Noninvasive in vivo photoacoustic measurement of internal jugular venous oxygenation in humans. arXiv Preprint. 2023;arXiv:2303.10775.
[18] Sangha GS, Hale NJ, Goergen CJ. Adjustable photoacoustic tomography probe improves light delivery and image quality. Photoacoustics 2018;12:6–13.
[19] Nguyen HNY, Steenbergen W. Reducing artifacts in photoacoustic imaging by using multi-wavelength excitation and transducer displacement. Biomed Opt Express 2019;10:3124–38.
[20] Jaeger M, Bamber JC, Frenz M. Clutter elimination for deep clinical optoacoustic imaging using localised vibration tagging (LOVIT). Photoacoustics 2013;1:19–29.
[21] Petrosyan T, Theodorou M, Bamber J, Frenz M, Jaeger M. Rapid scanning wide-field clutter elimination in epi-optoacoustic imaging using comb LOVIT. Photoacoustics 2018;10:20–30.
[22] Alles EJ, Jaeger M, Bamber JC. Photoacoustic clutter reduction using short-lag spatial coherence weighted imaging. In: Paper presented at: 2014 IEEE International Ultrasonics Symposium; 2014. p. Chicago, IL USA41–4.
[23] Schwab HM, Beckmann MF, Schmitz G. Photoacoustic clutter reduction by inversion of a linear scatter model using plane wave ultrasound measurements. Biomed Opt Express 2016;7:1468–78.
[24] Riksen JJ, Chandramoorthi S, van der Steen AF, van Soest G. Near-infrared multispectral photoacoustic analysis of lipids and intraplaque hemorrhage in human carotid artery atherosclerosis. Photoacoustics 2024;38:100636.
[25] Chandramoorthi S, Riksen JJ, Nikolaev AV, van der Steen AF, van Soest G. Wideband photoacoustic imaging in vivo with complementary frequency conventional ultrasound transducers. Front Phys 2022;10:954537.
[26] Daeichin V, Wu M, De Jong N, van der Steen AF, van Soest G. Frequency analysis of the photoacoustic signal generated by coronary atherosclerotic plaque. Ultrasound Med Biol 2016;42:2017–25.